Pharmaceutical Research, Vol. 23, No. 5, May 2006 (© 2006)
DOI: 10.1007/s11095-006-9909-1

Research Paper

A Novel *in Vitro* Percutaneous Penetration Model: Evaluation of Barrier Properties with *P*-Aminobenzoic Acid and Two of Its Derivatives

Miranda de Jager,[1] Wouter Groenink,[1] Ruth Bielsa i Guivernau,[2] Elin Andersson,[3] Nadezhda Angelova,[1] Maria Ponec,[4] and Joke Bouwstra[1,5]

Received November 17, 2005; accepted January 6, 2006

Purpose. The objective of this study was to evaluate the utility of a stratum corneum substitute (SCS) as a novel *in vitro* percutaneous penetration model. The SCS consists of synthetic stratum corneum (SC) lipids (cholesterol, free fatty acids, and specific ceramides) applied onto a porous substrate. The composition, organization, and orientation of lipids in the SCS bear high resemblance to that of the intercellular barrier lipids in SC.
Methods. The barrier integrity of the SCS was evaluated by means of passive diffusion studies, using three model compounds with different lipophilicities. The effects of lipid layer thickness, permeant lipophilicity, and altered lipid composition on the barrier properties were investigated, using isolated human SC as a control sample.
Results. For all three model compounds, the permeability characteristics of the SCS with a 12-μm-thick lipid layer closely resemble those of human SC. Modification of the lipid composition, generating an SCS that lacks the characteristic long periodicity phase as present in SC, was accompanied by a 2-fold increased permeability.
Conclusions. The SCS offers an attractive tool to predict solute permeation through human skin. Moreover, as its lipid composition can be modified, they may also serve as a suitable screening model for diseased skin.

KEY WORDS: barrier function; diffusion model; percutaneous penetration; stratum corneum; synthetic ceramides.

INTRODUCTION

For many years, the delivery of drugs into and through the skin has been an important area for research. Because of the natural function of the skin, however, only a limited number of drugs are capable to cross the outer layer of the skin, the stratum corneum (SC). The SC consists of several layers of partially overlapping corneocytes, which are surrounded by a cell envelope and are imbedded in a lipid matrix. Because of the highly impermeable character of the cornified envelope, substances that penetrate the SC bypass the corneocytes and follow the tortuous intercellular pathway (1–3). As a result, the SC lipids provide the actual barrier to the diffusion of substances through the skin. The lipid lamellae, which are oriented approximately parallel to the surface of the corneocytes (4,5), are predominantly composed of ceramides, cholesterol, and free fatty acids. It has been demonstrated that these stacks of crystalline lipid layers have repeating patterns of approximately 13 nm (long periodicity phase, LPP) and 6 nm (short periodicity phase, SPP), respectively (6–8). In particular, the LPP is considered to play a crucial role for proper skin barrier function.

At present, the most common means to screen transdermal and dermal drug delivery systems is the use of epidermis or SC, isolated from excised human or animal skin. However, those studies are hampered by the scarcity of human tissue and high intra- and interindividual variability of human and animal skin. Although animal skin is frequently used for permeation studies, its anatomical properties differ greatly from those of human skin. Because of the presence of numerous hair follicles and sebaceous glands, deviating composition and organization of the intercellular SC lipids and SC thickness, skin permeability cannot always be predicted adequately when using animal skin (9–11). Moreover, there will be an EU-wide ban on the use of animal skin in the testing of cosmetic products from 2009.

[1] Department of Drug Delivery Technology, Leiden/Amsterdam Center for Drug Research, University of Leiden, PO Box 9052, 2300 RA Leiden, The Netherlands.
[2] Department of Physico-Chemistry, Faculty of Pharmacy, University of Barcelona, Barcelona, Spain.
[3] Department of Pharmacy, University of Uppsala, Uppsala, Sweden.
[4] Department of Dermatology, Leiden University Medical Center, Leiden, The Netherlands.
[5] To whom correspondence should be addressed. (e-mail: bouwstra@chem.leidenuniv.nl)

The quest to circumvent these problems has prompted an extensive search for novel reliable *in vitro* penetration models. A few studies described the formation of model membranes by using lipids extracted from pig SC on a porous substrate (12,13). However, such an approach does not obviate the variability of native tissue and the laborious and time-consuming isolation and separation of the SC lipids. Accordingly, membranes prepared with isolated ceramides cannot be used for large-scale screening studies. Model membranes have also been prepared with the commercially available bovine brain ceramide type III or IV (14–19). Although the available information in literature about their use as a percutaneous penetration model is somewhat limited, the transport of water and some permeants across those model membranes seems to be similar to that across SC (16–18). However, it has been demonstrated that the lipid organization in those lipid membranes does not resemble that of SC (19–21). Moreover, no data on the orientation of the lamellae have been reported.

Obviously, the skin lipid membranes reported in literature do not meet all requirements for a reliable *in vitro* screening system to substitute for SC in diffusion studies. In a previous study, we developed a method to reproducibly produce a stratum corneum substitute (SCS) composed of cholesterol, long-chain free fatty acids, and specific synthetic ceramides on a porous substrate (22). The SCS was characterized in terms of uniformity of the lipid layer, distribution of the various lipid classes over the substrate surface, and the orientation and organization of the lipid lamellae (22). To the best of our knowledge, that was the first study in which a SCS was prepared that resembles the composition, organization, and orientation of the intercellular lipid lamellae in SC.

The aims of the present study were to evaluate the barrier properties of this SCS and to explore the possibility of using it as a novel predictive *in vitro* skin barrier model. These were accomplished by means of passive diffusion studies, using flow-through diffusion chambers, with *p*-aminobenzoic acid (PABA), ethyl-PABA, and butyl-PABA as model compounds and isolated human SC as a control sample. PABA is the most hydrophilic compound, and its lipophilicity increases with increasing ester chain length (see Table I). We aimed to answer the following questions:

(i) What is the effect of layer thickness on the diffusion profile?
(ii) What is the effect of permeant lipophilicity on the diffusion profile?
(iii) Is the presence of the LPP crucial for a proper permeability barrier?

Table I. Compounds Used in the Present Study

	PABA	Ethyl-PABA	Butyl-PABA
MW (g/mol)	137.1	165.2	193.2
$\text{Log}P_{\text{oct/H}_2\text{O}}$	0.58	1.44	2.61
C_d (mg/mL)	6.16	0.65	0.05

PABA = *p*-aminobenzoic acid.

MATERIALS AND METHODS

Materials

CER(EOS)C30, CER(NS)C24, CER(NP)C24, CER(NP)C16, CER(AS)C24, and CER(AP)C24 were generously provided by Cosmoferm B.V. (Delft, the Netherlands). The ceramides (CER) are composed of a long-chain sphingosine (S) or phytosphingosine (P) base with variations in the position and number of hydroxyl groups and double bonds. Through amide bonding, long-chain nonhydroxy (N) or α-hydroxy fatty acids (A) with a uniform acyl chain length (24 or 16 hydrocarbon atoms) are linked to the sphingoid bases. The exception is CER(EOS), which contains an ω-hydroxy fatty acid with a chain length of 30–32 carbon atoms to which linoleic acid is linked (EO) (23).

PABA, ethyl-PABA, and butyl-PABA, trypsin (type III, from bovine pancreas), and trypsin inhibitor (type II-S from soybean) were purchased from Sigma-Aldrich (Zwijndrecht, The Netherlands). Dialysis membrane disks (cutoff value of 5000 Da) were purchased from Diachema (Munich, Germany). Nuclepore polycarbonate filter disks (pore size 50 nm) were purchased from Whatman (Kent, UK). All organic solvents used were of analytical grade and manufactured by Labscan Ltd. (Dublin, Ireland). All other chemicals were of analytical grade. All aqueous solutions were prepared with Millipore water (Billerica, MA, USA).

Isolation of SC from Human Skin

SC was isolated from abdominal or mammary skin, which was obtained within 24 h after cosmetic surgery. After removal of the subcutaneous fat tissue, the skin was dermatomed to a thickness of approximately 250 μm using a Padgett Electro Dermatome Model B (Kansas City, KS, USA). The SC was separated from the epidermis by trypsin digestion [0.1% in phosphate-buffered saline (PBS), pH 7.4], after overnight incubation at 4°C and subsequently at 37°C for 1 h. The SC was then placed in a 0.1% solution of trypsin inhibitor and rinsed twice with Millipore water. Until use, the SC was stored in a silica-containing box under gaseous nitrogen in the dark to prevent oxidation of the intercellular SC lipids.

Preparation of SCS

The components for the synthetic ceramide mixtures were CER(EOS), CER(NS)C24, CER(NP)C24, CER(AS)C24, CER(NP)C16, and CER(AP)C24 in a molar ratio 15:51:16:4:9:5 (22,24). This lipid composition closely resembles the ceramide composition in pig SC (25). For the preparation of the free fatty acids mixtures, the following fatty acids were used: C16:0, C18:0, C20:0, C22:0, C23:0, C24:0, and C26:0 at molar ratios of 1.3, 3.3, 6.7, 41.7, 5.4, 36.8, and 4.7, respectively. This is similar to the composition of the free fatty acids in SC (26). Appropriate amounts of individual lipids dissolved in chloroform/methanol (2:1) were combined to yield lipid mixtures at the desired equimolar composition of cholesterol, synthetic ceramides, and free fatty acids. After evaporation of the organic solvent under a stream of

nitrogen, the lipid mixtures were redissolved in hexane/ethanol (2:1) at a total lipid concentration of 4.5 mg/mL. An evolution solo airbrush (Airbrush Service Almere, Lelystad, The Netherlands) was used to spray the lipid mixtures onto a polycarbonate filter disk with a pore size of 50 nm. Briefly, the substrate was mounted in a holder and fixed under the airbrush, which was constructed vertically with the nozzle facing downward. The reservoir of the airbrush was subsequently filled with lipid solution. During the spraying period, the trigger of the airbrush was opened pneumatically for a certain adjustable time period, during which a small fraction of the lipid solution passed the nozzle. Because of this nitrogen pressure, the lipid solution was sprayed in very small droplets onto the porous substrate. During the drying stage, the trigger was closed, the organic solvent evaporated by the nitrogen flow, and the lipids attached to the substrate. The number of spraying and drying cycles was adjustable to obtain the required layer thickness. The lipid-loaded filters were held at 70°C for 10 min and subsequently cooled to room temperature, after which the lipid organization closely resembles that in human SC (22).

Diffusion Studies

In vitro permeation studies were performed using Permegear in-line diffusion cells (Bethlehem, PA, USA) with a diffusion area of 0.28 cm^2. SC on a supporting dialysis membrane (apical side facing the donor chamber) or the SCS was mounted in the diffusion cell and was hydrated for 1 h in PBS (pH 7.4) prior to the experiment. The donor compartment was filled with 1280 µl of the drug solution in acetate buffer (pH 5.0) at saturated concentrations to obtain equal thermodynamic activities. The acceptor compartment consisted of PBS (pH 7.4), which was perfused at a flow rate of about 2 mL/h. The exact volume per collected fraction was determined by weighing. Each experiment was performed under occlusive conditions, by closing the opening of the donor compartment with adhesive tape. The temperature of the SC or SCS was maintained at 32°C during the total length of the experiment, using a thermostated water bath. Fractions were collected for 20 h at a 1-h interval. At the end of each experiment, the recovery was determined according to the following equation:

$$\text{Recovery} = [(\text{amount penetrated} + \text{amount remaining in donor compartment}) / \text{initial amount in donor compartment}]^{*}100\%$$

Influence of Compound Lipophilicity on the Diffusion Profile Across SC

Transport studies were performed across isolated human SC from four different donors. PABA, ethyl-PABA, and butyl-PABA were used as model compounds (see Table I). Each experiment was performed with SC originating from one donor, using six diffusion cells (i.e., two cells were used per test compound).

Influence of Layer Thickness on the Diffusion Profile Across SC

To assess the effect of the SC thickness on the diffusion profile of ethyl-PABA, the diffusion was measured across (a) a single SC sheet, (b) two SC sheets laid on top of each other, or (c) three SC sheets placed on top of each other. Each experiment was performed with SC originating from one donor, using six diffusion cells (i.e., two cells were used per layer thickness). SC derived from four different donors was used per experimental condition.

Influence of Lipid Layer Thickness on the Diffusion Profile Across the SCS

Diffusion profiles of ethyl-PABA were measured across the SCS, prepared with 160, 230, 350, and 420 µg of lipid material in the diffusion area. Six lipid-loaded filters were prepared and used per condition.

Influence of Compound Lipophilicity on the Diffusion Profile Across the SCS

Transport studies were performed across lipid-loaded filters, covered with approximately 350 µg of lipid in the diffusion area. PABA, ethyl-PABA, and butyl-PABA were used as model compounds. Each experiment was performed with six diffusion cells (i.e., two cells were used per compound). The experiment was performed in triplicate.

Influence of Altered Lipid Composition on the Diffusion Profile Across the SCS

Diffusion profiles of ethyl-PABA were measured across the SCS, prepared with two ceramide mixtures, either containing or not containing CER(EOS). Each experiment was performed with six diffusion cells. In three diffusion cells, the SCS that was prepared with ceramide mixtures lacking CER(EOS) was mounted, whereas the other three cells served as a control sample and contained the SCS prepared with ceramide mixtures containing CER(EOS). The experiment was performed in duplicate.

High-Performance Liquid Chromatographic Analysis

The samples were analyzed using a reverse-phase high-performance liquid chromatographic (HPLC) assay. The HPLC system consisted of a SP8810 LC pump (Spectra-Physics, Mountain View, CA, USA) equipped with a Gilson 234 autoinjector and UV-detector (Spectra-Physics UV150). A microparticulated C-18 column (Varian, Harbor City, CA; Chromosper C-18, 100 × 3.0 mm) was used as stationary phase. The mobile phase for ethyl-PABA and butyl-PABA consisted of acetonitrile and water in a ratio of 40:60. Acetonitrile, water, and acetic acid solution in a ratio of 20:78:2 was used as a mobile phase for PABA. The flow rate and the detection wavelength were set to 1.0 mL/min and 286 nm, respectively. A series of standards was run with each series of samples.

Data Analysis

The flux and cumulative amount of the model compounds were plotted as a function of time. Steady-state flux values (J_{ss}) were determined from the linear portions of the individual cumulative amount *vs.* time plot. The lag time (t_{lag}) was determined by extrapolation of this curve to the intercept with the time axis. Permeability coefficients (P) were calculated according to the equation $P = J_{ss}/C_d$, in which C_d is the concentration of the solute in the donor solution (in milligrams per cubic centimeter). Diffusion coefficients (D) were calculated from the slopes of the linear portions of the permeability coefficients *vs.* path length plots, according to the equation $P = KD/h$, in which K represents the partition coefficient of the permeant between the SC or SCS and the donor solution, D the diffusion coefficient of the permeant in the SC or SCS (in square centimeters per second), and h the length of the pathway through the SC or SCS (in centimeters).

All results are expressed as mean values ± standard deviations. Statistical analyses were performed using one-way ANOVA at a significance level set at $p < 0.05$. When a statistical analysis was performed for only two groups, an unpaired two-tailed t test was used.

Determination of the Amount and Thickness of the Lipid Layer on the Filter

After each diffusion experiment, the quantity of lipid material that was present in the diffusion area was determined. Briefly, the SCS was cut into two equally sized parts. One part was dissolved in 100 µl chloroform/methanol (2:1), and the lipids were extracted by extensive vortexing. After evaporation of the organic solvent, the amount of lipids was subsequently determined by weighing. The other part was used for cryo-scanning electron microscopy to establish the thickness of the lipid layer and to establish whether the SCS remains intact under the aqueous solutions used in the transport studies (22). Briefly, the lipid-loaded filters were cut into sheets of 1.5 × 2 mm^2, folded, and fixed in a small copper "shoe nail" using Tissue-Tek O.C.T. Compound (Miles Inc., Elkhart, IN, USA). The samples were then quickly frozen by plunge freezing (Reichert Jung-KF80, Vienna, Austria) into liquid propane at −180°C. The frozen specimens were kept in liquid nitrogen until mounting into a sample holder. The cryofixed samples were planed in a cryo ultramicrotome (Leica Ultracut UCT/Leica EM FCS, Wetzlar, Germany), using a specimen temperature of −90°C and a knife temperature of −100°C. Subsequently, the samples were vacuum dried for 3 min at −90°C at 0.1 Pa to obtain contrast and sputtered with a layer of platinum (CT 1500 HF, Oxford Instruments, UK). After transferring the specimens into the field emission scanning electron microscope (Jeol 6400F, Tokyo, Japan), the samples were analyzed at −190°C. At least four microscopic images were taken from each SCS, and three SCSs were examined per experimental condition. At equal distances of 20 µm along the cutting plane, the thickness of the cross section of each lipid layer was determined by establishing the pixel position of the top and bottom of the lipid layer in proportion to that of the magnification bar that is present in each micrograph.

RESULTS

Effect of Layer Thickness on the Diffusion Profile

To assure that the polycarbonate filter used for the generation of the SCS does not form an additional diffusion barrier, experiments were first carried out with lipid-free polycarbonate filters. The measured flux values of ethyl-PABA were approximately 15-fold higher (data not shown) than those measured across the SCS prepared with a 12-µm-thick lipid layer or isolated human SC, indicating that the polycarbonate filter does not act as an additional barrier. In addition, the flux values of ethyl-PABA across the supporting dialysis membranes were investigated. These seemed to be approximately 10-fold higher (data not shown) than those across SC.

Figure 1 shows the flux profiles of ethyl-PABA across SC and the SCS as a function of time. The average steady-state flux (J_{ss}) and lag time (t_{lag}) values obtained from the individual cumulative amount *vs.* time plots, together with the calculated permeability coefficient (P), are presented in Table II. The t_{lag} values obtained in these permeation experiments are quite variable, which is reflected by large standard deviations. An increase in the SC thickness by increasing the number of SC layers from one to three is accompanied by an almost 3-fold decrease in the J_{ss} and an almost 4-fold increase in the t_{lag}. For the SCS, it can also be observed that the flux is highly affected by the layer thickness. Plots of P *vs.* the reciprocal quantity of lipid material in the diffusion area (Fig. 2A) or P *vs.* the reciprocal layer thickness of the SCS

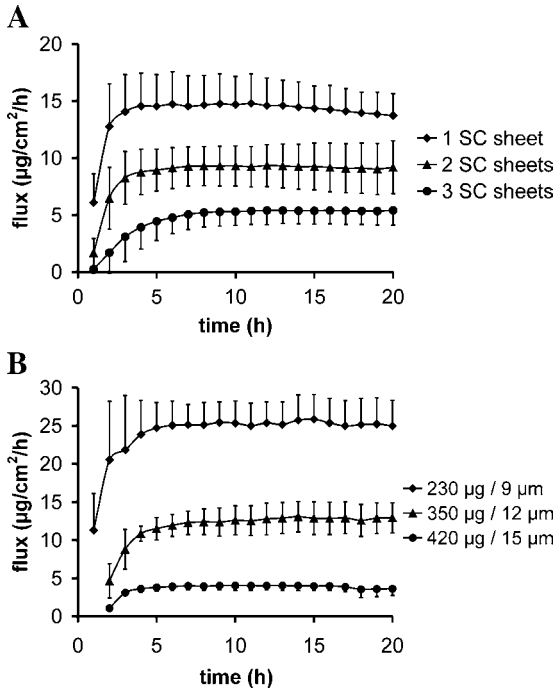

Fig. 1. Effect of layer thickness on the flux profiles of ethyl-*p*-aminobenzoic acid (ethyl-PABA) across isolated human stratum corneum (SC; A) and the stratum corneum substitute (SCS; B). An increased layer thickness is accompanied by a decrease in the steady-state flux. Data are presented as average ± SD ($n = 8$ for SC and $n = 6$ for the SCS).

Table II. Influence of Layer Thickness on Diffusion Characteristics of Ethyl-PABA

Parameter	1 SC sheet	2 SC sheets	3 SC sheets	SCS 160 μg/ 6 μm	SCS 230 μg/ 9 μm	SCS 350 μg/ 12 μm	SCS 420 μg/ 15 μm
J_{ss} (μg/cm^2/h)	14.6 ± 2.4	9.2 ± 1.9	5.4 ± 1.2	42.6 ± 4.5	26.4 ± 3.3	12.9 ± 2.1	4.0 ± 0.6
t_{lag} (h)	0.8 ± 0.4	1.3 ± 0.4	3.0 ± 1.4	0.8 ± 0.6	1.3 ± 1.0	1.4 ± 0.3	1.0 ± 0.3
P (cm/s)	$6.3 \times 10^{-6} \pm 1.0 \times 10^{-6}$	$4.0 \times 10^{-6} \pm 8.3 \times 10^{-7}$	$2.3 \times 10^{-6} \pm 5.2 \times 10^{-7}$	$1.8 \times 10^{-5} \pm 1.9 \times 10^{-6}$	$1.1 \times 10^{-5} \pm 1.4 \times 10^{-6}$	$5.5 \times 10^{-6} \pm 8.9 \times 10^{-7}$	$1.7 \times 10^{-6} \pm 2.5 \times 10^{-6}$
Recovery (%)	101.3 ± 7.0	100.7 ± 6.5	99.2 ± 7.4	95.6 ± 3.9	100.2 ± 8.1	97.6 ± 5.6	95.2 ± 3.1

The numbers provided with the SCS are the amount of lipid in the diffusion area and the lipid membrane thickness, respectively.
SC = stratum corneum; SCS = stratum corneum substitute.

(Fig. 2B) both have positive linear slopes and a correlation coefficient of 0.96, indicating that the steady-state diffusion across the SCSs is in accordance with Fick's law.

In contrast to the J_{ss}, no relationship is found between the lipid layer thickness of the SCS and the t_{lag}. Independent of the lipid layer thickness, an average t_{lag} of approximately 1 h is observed. It should be stressed, however, that very short t_{lag} values cannot be appropriately determined with the diffusion setup used in the present study. At a flow rate of 2 mL/h, it takes about 1 h to replace the acceptor fluid in the acceptor compartment and the connecting tubings to the fraction collector. As a result, the obtained t_{lag} values of ethyl-PABA across the SCS may not reflect the real situation.

The results of these experiments convincingly show that the diffusion profile of ethyl-PABA across the SCS can be regulated by means of its layer thickness. Diffusion profiles of ethyl-PABA across a single SC sheet bear high resemblance to the SCS prepared with approximately 350 μg of lipid material in the diffusion area. This quantity corresponds to a lipid layer thickness of approximately 12 μm (see also Figs. 2B and 5B).

Effect of Permeant Lipophilicity on the Diffusion Profile

Figures 3A and B show the flux *vs.* time profiles of the three model compounds across a single layer of SC and across the SCS prepared with approximately 350 μg of lipid material, respectively. In case of the SCS, a slight decrease in the J_{ss} of butyl-PABA can be observed after approximately 10 h, which is caused by depletion of the compound from the donor phase (Fig. 3B).

The average J_{ss} and t_{lag} values obtained from the individual cumulative amount *vs.* time plots, together with P, are presented in Table III. The diffusion profiles of the three compounds across the SCS and SC are very similar. For both SCS and SC, it can be observed that the t_{lag} of PABA is significantly longer than for the more lipophilic compounds ethyl-PABA and butyl-PABA. Furthermore, the t_{lag} of PABA across the SCS was found to be longer than that across SC. With respect to the t_{lag} of the other two model compounds, however, no significant differences are observed between the SCS and SC.

The results further reveal that the highest fluxes are obtained with the intermediate lipophilic ethyl-PABA. Increasing (butyl-PABA) or decreasing (PABA) the compound lipophilicity results in a significant decrease in the J_{ss}. The calculated P values indicate that the permeability of both SC and SCS increases with increasing compound

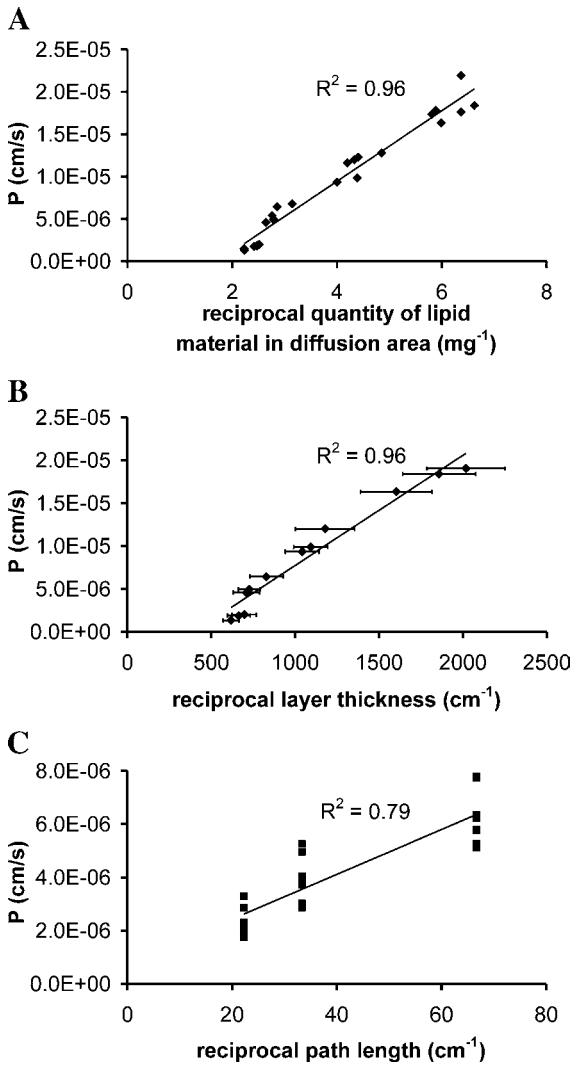

Fig. 2. (A) Relationship between the partition coefficient and the reciprocal quantity of lipid material in the diffusion area. (B) Relationship between the partition coefficient and the reciprocal layer thickness of the SCS. (C) Relationship between the partition coefficient and the reciprocal path length in SC. In accordance with Fick's first law of diffusion, the linear slope represents the diffusion coefficient multiplied with the partition coefficient. The reciprocal layer thickness values are presented as average ± SD. All lipid-loaded filters examined are still intact after the permeation studies and did not reveal the presence of any defects (open structures).

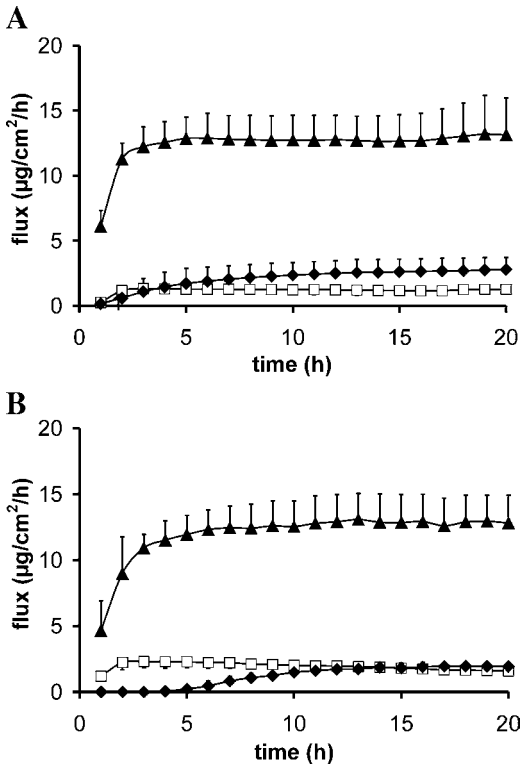

Fig. 3. Effect of permeant lipophilicity on the diffusion profile. Flux *vs.* time profiles of PABA (-♦-), ethyl-PABA (-▲-) and butyl-PABA (-□-) across SC (A) and the SCS prepared with approximately 350 µg lipid material in the diffusion area (B).

lipophilicity. For PABA and ethyl-PABA, no significant differences in P (or J_{ss}) are observed between the SCS and SC. Compared with SC, however, the SCS seems to be slightly more permeable to butyl-PABA, as can be derived from the nearly 2-fold higher P (and J_{ss}).

Effect of Altered Lipid Composition on the Diffusion Profile Across the SCS

To investigate the effect of altered lipid composition on the permeability barrier, the SCS was also prepared with ceramide mixtures lacking CER(EOS). From previous X-ray diffraction studies, it became evident that synthetic SC lipid mixtures prepared lacking CER(EOS) do not form the characteristic LPP (24,27). Figure 4 and Table IV show that the SCS prepared with mixtures lacking CER(EOS) show almost 2-fold higher J_{ss} values ($p < 0.01$) than the SCS prepared with CER(EOS). This indicates that the 13-nm lamellar phase, at least partially, contributes to the barrier integrity of the SCS.

DISCUSSION

Our overall goal is to develop a skin barrier model (consisting of a porous substrate covered with synthetic SC lipids), which mimics the lipid composition, lipid organization, lipid orientation, and permeability barrier of human SC. This SCS may ultimately function as an *in vitro* screening system pertaining to transdermal drug delivery. The main advantages of such a percutaneous penetration model are that (a) it is a well-defined system, (b) it circumvents problems related to human or animal skin, (c) it is easy to handle and can be mounted in a commercially available Permegear diffusion cell, and (d) the composition of the synthetic SC lipids can be manipulated, which offers the opportunity to mimic the lipid organization in healthy as well as in diseased skin.

In a previous study, we have already demonstrated that an airbrush is an elegant apparatus to apply smooth and tightly packed lipid membranes of uniform thickness onto a polycarbonate filter (22). Lipid analysis revealed that all lipids within the SCS are homogeneously distributed over the filter surface. The SCS further possesses two crystalline lamellar phases with periodicities of 12.2 and 5.4 nm, which are oriented parallel to the filter surface. Those results indicate that it is possible to prepare a SCS that closely resembles the lipid composition, organization, and orientation of the intercellular lipids in SC.

The present study investigated the permeability barrier of this SCS. The results convincingly show that the barrier properties of the SCS prepared with a 12-µm-thick lipid layer are very similar to those of isolated human SC. However, some items need to be discussed to evaluate the full potential of the SCS as a novel *in vitro* percutaneous penetration model, namely, (a) the differences in the penetration route between the SCS and SC, (b) the effect of permeant lipophilicity on the penetration profile, and (c) the effect of altered membrane composition on the permeability barrier of lipid membranes. Each of these items is discussed below.

Differences in Penetration Route Between SCS and SC

Diffusion profiles of ethyl-PABA across the SCS prepared with a 12-µm-thick lipid layer show high similarity to those obtained with isolated human SC. An increased layer thickness is accompanied by an increased barrier efficacy, which is reflected by a decrease in J_{ss}. However, an increased

Table III. Influence of Permeant Lipophilicity on Diffusion Characteristics Across SC and the SCS

Parameter	PABA SC	Ethyl-PABA SC	Butyl-PABA SC	PABA SCS	Ethyl-PABA SCS	Butyl-PABA SCS
J_{ss} (µg/cm²/h)	2.7 ± 1.0	12.5 ± 2.0	1.2 ± 0.3	2.0 ± 0.3	12.9 ± 2.1	2.2 ± 0.5
t_{lag} (h)	4.7 ± 1.7	0.7 ± 0.3	0.8 ± 0.6	7.4 ± 0.8	1.4 ± 0.3	0.7 ± 0.4
P (cm/s)	$1.2 \times 10^{-7} \pm 4.5 \times 10^{-8}$	$5.4 \times 10^{-6} \pm 8.5 \times 10^{-7}$	$7.2 \times 10^{-6} \pm 2.0 \times 10^{-6}$	$8.8 \times 10^{-8} \pm 1.2 \times 10^{-8}$	$5.5 \times 10^{-6} \pm 8.9 \times 10^{-7}$	$1.3 \times 10^{-5} \pm 2.6 \times 10^{-6}$
Recovery (%)	n.d.	n.d.	n.d.	101.0 ± 1.1	97.6 ± 5.6	98.9 ± 3.4

n.d. = not determined.

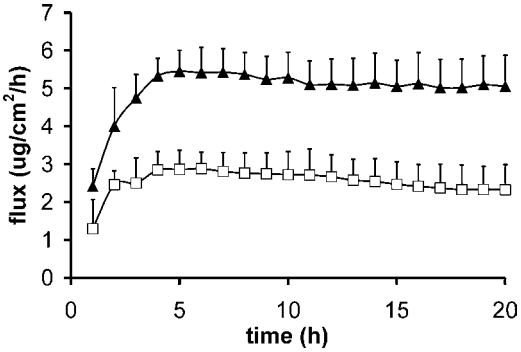

Fig. 4. Effect of altered lipid composition on the flux profiles of ethyl-PABA across the SCS, prepared with approximately 440 μg of lipid material in the diffusion area. The SCS prepared in the absence of CER(EOS) (-▲-) does not reveal the long periodicity phase. The reduced barrier efficacy of this SCS is reflected by a 2-fold increase in the steady-state flux as compared with the SCS prepared in the presence of CER(EOS) (-□-). Data are presented as average ± SD ($n = 6$).

layer thickness does not result in an increased t_{lag}, which is different from the observations made with SC. It is therefore of interest to compare the organization of the synthetic lipids in the SCS with the intercellular lipids in SC.

Difference in Number of Lipid Lamellae

SC consists of approximately 15 layers of partially overlapping corneocytes (28). When the assumptions are made that (a) six lamellae are present between two adjacent corneocytes and (b) the re-peat distance of these lamellae is 13 nm, it can be calculated that the total thickness of the intercellular lipid lamellae in SC is approximately 1.2 μm (3). This is 10-fold smaller than the thickness of the lipid layer in the SCS, being approximately 12 μm. When the quantity of lipid material present per unit area in SC and the SCS is compared, again a nearly 10-fold difference is observed. Whereas the SCS is composed of approximately 350 μg lipid material in the diffusion area, SC only contains approximately 30 μg lipids. This latter calculation is based on the assumptions that (a) ceramides, cholesterol, and free fatty acids account for 10% of the SC dry weight (3), (b) the density of SC is 1 g/cm^3, and (c) the thickness of dry SC is 10 μm (29).

Difference in Penetration Path Length

Another difference between SC and the SCS is the penetration path length, h. Figure 5A shows a cryo-scanning electron microscopy photo of isolated human SC, hydrated in PBS. SC contains corneocytes, which are all surrounded by a very impermeable cornified envelope. As a result, compounds that penetrate the SC do not traverse the interior of the corneocytes but follow the tortuous path along the corneocytes (1–3). Based on this principle, Talreja *et al.* (29) calculated the tortuous lipid path length in alkali-expanded human SC from arbitrary points on the SC surface to the viable epidermis. Based on their results, average path lengths of 180 and 130 μm are reported for alkali-expanded and dry SC, respectively. As the alkaline expansion technique produces swelling of the SC comparable to that obtained with full hydration (29), 150 μm has been advocated as a realistic penetration path length in PBS hydrated SC, used in the present study.

In contrast to SC, the SCS is solely composed of synthetic lipids and does not contain corneocytes. We hypothesize that the path length in the SCS is perpendicular to the lipid membrane surface, rather than tortuous, and therefore equal to the thickness of the lipid layer, being approximately 12 μm. As compounds may not only diffuse perpendicularly to the lipid lamellae but also parallel to the lipid lamellae, the actual path length in both the SCS and SC might be considerably longer than the proposed 150 and 12 μm. In fact, to bypass the corneocytes in the SC, a compound already needs to diffuse laterally to some extent. For instance, through mathematical modeling, Johnson *et al.* (3) calculated that the effective tortuosity in SC (i.e. taking into account parallel diffusion) is approximately 3.6 cm.

Difference in Diffusion Coefficient

Figure 2C shows the relationship between the calculated permeability coefficient in SC and the reciprocal penetration path length, assuming an intercellular path length of 150, 300, and 450 μm in one, two, and three SC sheets, respectively. From the slope of the linear portions of Fig. 2B and C, the diffusion coefficient D was calculated. For these calculations, the partition coefficient of ethyl-PABA between the SC or lipid membranes and the donor solution is assumed to be equal to the octanol-to-water partition coefficient of ethyl-PABA. The diffusion coefficient in the SCS ($D = 4.7 \times 10^{-10}$ cm^2/s) is nearly 6-fold smaller than that in SC ($D = 2.7 \times 10^{-9}$ cm^2/s). This indicates that, despite the shorter path length in the SCS, the mobility of ethyl-PABA is lower than that in SC, assuming that the estimated penetration path lengths in SC and SCS are correct. A possible explanation for the lower diffusion coefficient in the SCS is that ethyl-PABA has to cross 10-fold more lamellae, as the total thickness of the SCSs is 10-fold larger than that in SC. Moreover, the corneocytes and adjacent lamellae in SC are not exactly running parallel to the skin surface. As a result, the penetration into the SC is not only affected by diffusion perpendicular to the lipid lamellae but also by diffusion parallel to the lipid lamellae (illustrated in Fig. 5C). We would like to emphasize that the

Table IV. Influence of Altered Lipid Composition of SCSs on Diffusion Characteristics of Ethyl-PABA

Parameter	SCS prepared in the presence of CER(EOS)	SCS prepared in the absence of CER(EOS)
J_{ss} (μg/cm^{-2}/h^{-1})	2.7 ± 0.4	5.2 ± 0.7
t_{lag} (h)	0.6 ± 0.4	0.8 ± 0.6
P (cm/s)	$1.2 \times 10^{-6} \pm 1.8 \times 10^{-7}$	$2.2 \times 10^{-6} \pm 3.2 \times 10^{-7}$
Recovery (%)	97.8 ± 9.1	94.9 ± 3.0

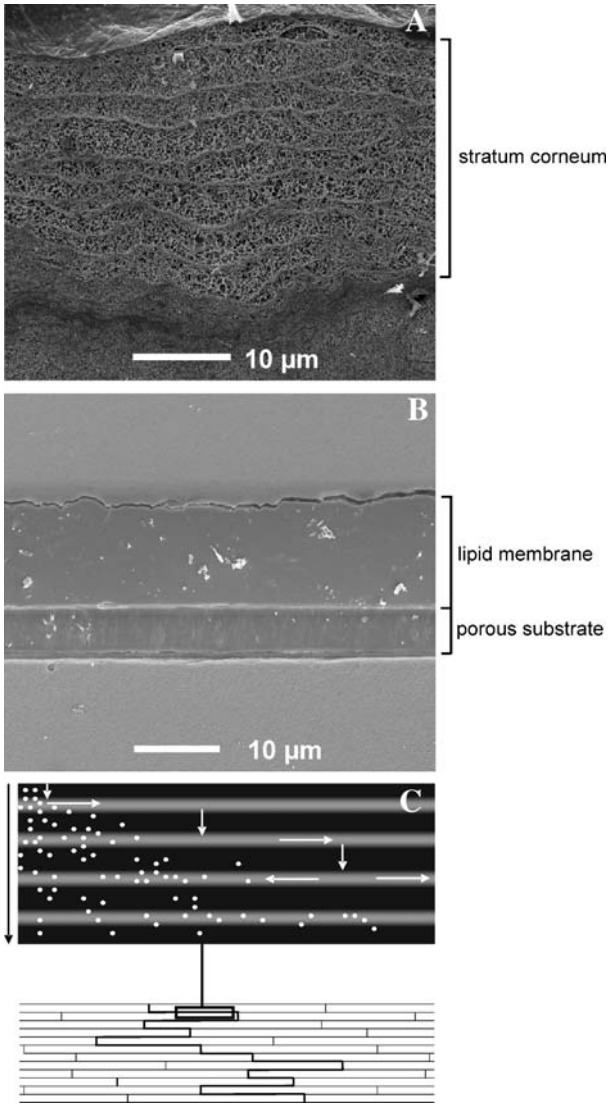

Fig. 5. Cryo-scanning electron microscopy photos of isolated human SC, hydrated in phosphate-buffered saline (A), and the SCS after a permeation experiment (B). Schematic representation of SC and parallel diffusion (C). The wall-like structure represents the partially overlapping corneocytes (bricks) and the surrounding lipids (mortar). The thick line illustrates a possible penetration route which a substance may take to travel from the SC surface to the viable epidermis. However, as parallel diffusion of molecules within the stacks of lamellae is possible (see magnification), the actual path length may be considerably increased. The black vertical arrow indicates the concentration gradient.

diffusion rate parallel to the lipid lamellae may be higher than the diffusion rate perpendicular to the lipid lamellae, as in the latter a compound has to pass alternately lipophilic and hydrophilic domains.

In contrast to the SCS, native SC contains appendages, such as sweat glands and hair follicles with their associated sebaceous glands. As the appendages only represent approximately 0.1% of the total skin area (30), for passive diffusion the transappendageal route is frequently considered to be less important than the transepidermal route. The results of the present study reveal that pores as remnants of the transappendageal route, which may be present in the diffusion area of the isolated SC pieces, do not contribute significantly to the transport of ethyl-PABA. Pores that might be present in the SC pieces are blocked when two or more SC sheets are placed on top of each other. When pores would play a significant role in the diffusion of ethyl-PABA across SC, a nonlinear decrease in the permeability coefficient is expected (31). However, as a linear relationship is obtained between the permeability coefficient and the reciprocal path length (see Fig. 2C), pores are not considered to contribute significantly to the transport of ethyl-PABA through SC. Moreover, constant relative standard deviations are found for J_{ss} and t_{lag} of ethyl-PABA across one, two, or three SC sheets.

Effect of Permeant Lipophilicity on the Permeability Coefficient in SCS is Similar to that in SC

The results of the present study show that the permeability coefficients of PABA, ethyl-PABA, and butyl-PABA in the SCS prepared with a 12-µm-thick lipid layer closely resemble those in SC. This means that the SCS has very similar permeability characteristics as human SC. It has further been demonstrated that the permeability coefficient increases in the order PABA < ethyl-PABA < butyl-PABA (see Table III). This is consistent with literature data obtained with human or hairless mouse skin, in which a linear relationship between the permeability and the lipophilicity of homologous *n*-alkanols or hydrocortisone-21 esters is reported until a plateau is reached (32,33).

The SCS seems to be slightly more permeable to the most lipophilic compound butyl-PABA. However, the observed differences in P and J_{ss} are maximally 2-fold, which are much smaller than reported for other compounds when using animal or *in vitro* reconstructed skin to replace human SC (10,11,34–36). Differences in the permeability between SC and the SCS may be explained by differences in the lipid composition. The SCS is composed solely of synthetic ceramides, cholesterol, and free fatty acids, whereas SC also contains more hydrophilic lipids, in particular in the deepest layers. This may also explain the slightly increased t_{lag} of PABA through the SCS as compared with SC. The barrier properties of the SCS to extremely lipophilic and hydrophilic compounds, including water, remain to be elucidated.

Alteration of Lipid Composition of SCS Affects Solute Permeation

The LPP is always considered to play an important role in the skin barrier function. To date, however, no direct evidence is available from permeability studies that this is indeed the case. One of the major advantages of the SCS is that the composition of the lipid mixtures can be accurately chosen and modified. This offers excellent opportunities to systemically investigate the role of each lipid subclass for proper lipid organization and barrier function. The results of the present study show that the SCS prepared with a ceramide mixture lacking CER(EOS) is more permeable to solute permeation than the SCS prepared in the presence of CER(EOS). In previous studies, it has been established that lipid mixtures lacking CER(EOS) do not form the LPP

(24,27). These results demonstrate that the LPP contributes to the barrier integrity of the SCS. In certain skin disorders, such as psoriasis and atopic dermatitis, a marked reduction of CER(EOS) in the lesion parts of the SC is observed (23,37–40). Extrapolation of the present results to the *in vivo* situation suggests that the observed barrier malfunction in these skin diseases can at least in part be explained by a reduced formation of the LPP.

Ultimately, an SCS may be generated that imitates the lipid composition and organization as observed in various skin diseases. Such studies are of crucial importance to elucidate the relationship between lipid composition, organization, and barrier function. Moreover, this may provide unique possibilities to more adequately predict the permeation of drug substances through diseased skin, for which there is currently no alternative.

CONCLUSION

The results of the present study convincingly show that the SCS prepared with cholesterol, free fatty acids, and specific synthetic ceramides can successfully be used to predict solute permeation through the skin. The barrier properties of the SCS can easily be adjusted by applying different amounts of lipids or by modifying its lipid composition, mimicking that of diseased skin. This demonstrates that this novel SCS has a great potential to be used in screening studies. However, further studies are required to investigate the barrier properties of the SCS to other compounds and different formulations, including those with penetration enhancers.

ACKNOWLEDGMENTS

This work was supported by a grant from the Technology Foundation STW (LGN4654). The authors would like to thank the Center for Electron Microscopy (Leiden University Medical Center) and the Department of Plant Sciences (Wageningen University) for the use of their electron microscopy facilities.

REFERENCES

1. H. E. Boddé, I. van der Brink, H. K. Koerten, and F. H. N. Haande. Visualization of *in vitro* percutaneous penetration of mercuric chloride transport through intercellular space *versus* cellular uptake through desmosomes. *J. Control. Release* **15**: 227–236 (1991).
2. M. E. M. J. Meuwissen, J. Janssen, C. Cullander, H. E. Junginger, and J. A. Bouwstra. A cross-section device to improve visualization of fluorescent probe penetration into the skin by confocal laser scanning microscopy. *Pharm. Res* **15**: 352–356 (1998).
3. M. E. Johnson, D. Blankschtein, and R. Langer. Evaluation of solute permeation through the stratum corneum: lateral bilayer diffusion as the primary transport mechanism. *J. Pharm. Sci* **86**: 1162–1172 (1997).
4. K. C. Madison, D. C. Schwartzendruber, P. W. Wertz, and D. T. Downing. Presence of intact intercellular lipid lamellae in the upper layers of the stratum corneum. *J. Invest. Dermatol.* **88**: 714–718 (1987).
5. D. C. Schwartzendruber, P. W. Wertz, D. J. Kitko, K. C. Madison, and D. T. Downing. Molecular models of intercellular lipid lamellae in mammalian stratum corneum. *J. Invest. Dermatol.* **92**:251–257 (1989).
6. J. A. Bouwstra, G. S. Gooris, J. A. van der Spek, and W. Bras. The structure of human stratum corneum as determined by small angle X-ray scattering. *J. Invest. Dermatol* **96**:1006–1014 (1991).
7. J. A. Bouwstra, G. S. Gooris, J. A. van der Spek, and W. Bras. Structural investigations of human stratum corneum by small angle X-ray scattering. *J. Invest. Dermatol.* **97**:1005–1012 (1991).
8. J. A. Bouwstra, G. S. Gooris, W. Bras, and D. T. Downing. Lipid organization in pig stratum corneum. *J. Lipid Res.* **36**:685–695 (1995).
9. C. R. Behl, G. L. Flynn, T. Kurihara, W. Smith, W. I. Higuchi, N. F. W. Ho, and C. L. Pierson. Hydration and percutaneous absorption: I. Influence of hydration on alcohol permeation through hairless mouse skin. *J. Invest. Dermatol.* **75**:346–352 (1980).
10. P. Catz and D. R. Friend. Transdermal delivery of levonorgestrel. VII. Effect of enhancers on rat skin, hairless mouse skin, hairless guinea pig skin, and human skin. *Int. J. Pharm.* **58**:93–102 (1990).
11. F. P. Schmook, J. G. Meingassner, and A. Billich. Comparison of human skin or epidermis models with human and animal skin in *in-vitro* percutaneous absorption. *Int. J. Pharm.* **215**:51–56 (2001).
12. S. E. Friberg, I. Kayali, W. Beckerman, L. D. Rhein, and A. Simion. Water permeation of reaggregated stratum corneum with model lipids. *J. Invest. Dermatol.* **94**:377–380 (1990).
13. D. Kuempel, D. C. Swartzendruber, C. A. Squier, and P. W. Wertz. *In vitro* reconstitution of stratum corneum lipid lamellae. *Biochim. Biophys. Acta* **1372**:135–140 (1998).
14. W. Abraham and D. T. Downing. Preparation of model membranes for skin permeability studies using stratum corneum lipids. *J. Invest. Dermatol.* **93**:809–813 (1989).
15. S. E. Friberg and I. Kayali. Water evaporation rates from a model of stratum corneum lipids. *J. Pharm. Sci.* **78**:639–643 (1989).
16. D. Kittayanond, S. M. Dowton, C. Ramachandran, G. L. Flynn, and N. Weiner. Development of a model of the lipid constituent phase of the stratum corneum: II. Preparation of artificial membranes from synthetic lipids and assessment of permeability properties using *in vitro* diffusion experiments. *J. Soc. Cosmet. Chem.* **43**:237–249 (1992).
17. K. Matsuzaki, T. Imaoka, M. Asano, and K. Miyajima. Development of a model membrane system using stratum corneum lipids for estimation of drug skin permeability. *Chem. Pharm. Bull.* **41**:575–579 (1993).
18. K. Miyajima, S. Tanikawa, M. Asano, and K. Matsuzaki. Effects of absorption enhancers and lipid composition on drug permeability through the model membrane using stratum corneum lipids. *Chem. Pharm. Bull.* **42**:1345–1347 (1994).
19. R. Lieckfeldt, J. Villalain, J. C. Gomez-Fernandez, and G. Lee. Diffusivity and structural polymorphism in some model stratum corneum lipid systems. *Biochim. Biophys. Acta* **1151**:182–188 (1993).
20. J. A. Bouwstra, J. Thewalt, G. S. Gooris, and N. Kitson. A model membrane approach to the epidermal permeability barrier: an X-ray diffraction study. *Biochemistry* **36**:7717–7725 (1997).
21. M. W. de Jager, G. S. Gooris, I. P. Dolbnya, W. Bras, M. Ponec, and J. A. Bouwstra. The phase behaviour of skin lipid mixtures based on synthetic ceramides. *Chem. Phys. Lipids* **124**:123–134 (2003).
22. M. W. de Jager, G. S. Gooris, M. Ponec, and J. A. Bouwstra. Preparation and characterization of a stratum corneum substitute for *in vitro* percutaneous penetration studies. *Biochim. Biophys. Acta*, in press.
23. S. Motta, M. Monti, S. Sesana, R. Caputo, S. Carelli, and R. Ghidoni. Ceramide composition of the psoriatic scale. *Biochim. Biophys. Acta* **8**:147–151 (1993).
24. M. W. de Jager, G. S. Gooris, M. Ponec, and J. A. Bouwstra. Lipid mixtures prepared with well-defined synthetic ceramides closely mimic the unique stratum corneum lipid organization. *J. Lipid Res.* **46**:2649–2656 (2005).

25. J. A. Bouwstra, G. S. Gooris, K. Cheng, A. Weerheim, W. Bras, and M. Ponec. Phase behavior of isolated skin lipids. *J. Lipid Res.* **37**:999–1011 (1999).
26. P. W. Wertz and D. T. Downing. Epidermal lipids. In L. A. Goldsmith (ed)., *Physiology, Biochemistry and Molecular Biology of the Skin*, Oxford University Press, Oxford, 1991, pp. 205–235.
27. M. de Jager, G. Gooris, M. Ponec, and J. Bouwstra. Acylceramide head group architecture affects lipid organization in synthetic ceramide mixtures. *J. Invest. Dermatol.* **123**:911–916 (2004).
28. Z. Ya-Xian, T. Suetake, and H. Tagami. Number of cell layers of the stratum corneum in normal skin—relationship to the anatomical location on the body, age, sex and physical parameters. *Arch. Dermatol. Res.* **291**:555–559 (1999).
29. P. S. Talreja, G. B. Kasting, N. K. Kleene, W. L. Pickens, and T. F. Wang. Visualization of the lipid barrier and measurement of lipid pathlength in human stratum corneum. *AAPS PharmSci* **3**(Article 13):1–9 (2001).
30. B. W. Barry. Structure, function, diseases, and topical treatment of human skin. In *Dermatological Formulations: Percutaneous Absorption*, Marcel Dekker, New York, 1983, pp. 1–48.
31. E. A. Essa, M. C. Bonner, and B. W. Barry. Human skin sandwich for assessing shunt route penetration during passive and iontophoretic drug and liposome delivery. *J. Pharm. Pharmacol.* **54**:1481–1490 (2002).
32. S. E. Cross, B. M. Magnusson, G. Winckle, Y. Anissimov, and M. S. Roberts. Determination of the effect of lipophilicity on the *in vitro* permeability and tissue reservoir characteristics of topically applied solutes in human skin layers. *J. Invest. Dermatol.* **120**:759–764 (2003).
33. H. Schaefer and T. E. Redelmeier. *Skin Barrier. Principles of Percutaneous Absorption*, Karger, Basel, 1996.
34. N. Garcia, O. Doucet, M. Bayer, D. Fouchard, L. Zastrow, and J. P. Marty. Characterization of the barrier function in a reconstituted human epidermis cultivated in chemically defined medium. *Int. J. Cosmet. Sci.* **24**:25–34 (2002).
35. S. D. Roy, J. Fujiki, and J. S. Fleitman. Permeabilities of alkyl *p*-aminobenzoates through living skin equivalents and cadaver skin. *J. Pharm. Sci.* **82**:1266–1269 (1993).
36. H. Wagner, K. H. Kosta, K. M. Lehr, and U. F. Schaefer. Interrelation of permeation and penetration parameters obtained from *in vitro* experiments with human skin and skin equivalents. *J. Control. Release* **75**:283–295 (2001).
37. A. Di Nardo, P. Wertz, A. Giannetti, and S. Seidenari. Ceramide and cholesterol composition in the skin in patients with atopic dermatitis. *Acta Derm.-Venereol. (Stockh)* **78**:27–30 (1998).
38. R. Ghadially, J. T. Reed, and P. M. Elias. Stratum corneum structure and function correlates with phenotype in psoriasis. *J. Invest. Dermatol.* **107**:558–564 (1996).
39. A. Yamamoto, S. Serizaka, M. Ito, and Y. Sato. Stratum corneum lipid abnormalities in atopic dermatitis. *Arch. Dermatol. Res.* **283**:219–223 (1991).
40. A. P. M. Lavrijsen, J. A. Bouwstra, G. S. Gooris, H. E. Boddé, and M. Ponec. Reduced skin barrier function parallels abnormal stratum corneum lipid organisation in patients with lamellar ichthyosis. *J. Invest. Dermatol.* **105**:619–624 (1995).